

The effect of preparation conditions on the properties of $\text{Li}_3\text{V}_2(\text{PO}_4)_3$ cathode powders prepared by ultrasonic spray pyrolysis

You Na Ko, Jung Hyun Kim, Young Jun Hong and Yun Chan Kang*

Department of Chemical Engineering, Konkuk University, 1 Hwayang-dong, Gwangjin-gu, Seoul 143-701, Korea

$\text{Li}_3\text{V}_2(\text{PO}_4)_3$ powders were prepared by spray pyrolysis under various conditions of gas atmosphere, preparation temperature, and carrier gas flow rate. The precursor powders had a submicrometre size and spherical shape irrespective of their preparation conditions. The morphologies and crystal structures of subsequently post-treated powders varied with the preparation conditions: 1300 °C with a flow rate of 20 L minute⁻¹ under 10% H_2/N_2 reducing gas produced spherical, pure $\text{Li}_3\text{V}_2(\text{PO}_4)_3$ particles. $\text{Li}_3\text{V}_2(\text{PO}_4)_3$ powder prepared under the optimum conditions showed a maximum initial discharge capacity of 144 mAhg⁻¹.

Key words: Cathode material, Spray pyrolysis, Lithium vanadium phosphate.

Introduction

$\text{Li}_3\text{V}_2(\text{PO}_4)_3$ is a promising cathode material for lithium secondary batteries. The reversible cycling of each of its three lithium ions from $\text{Li}_3\text{V}_2(\text{PO}_4)_3$ would correspond to a theoretical capacity of 197 mAhg⁻¹ [1-4]. $\text{Li}_3\text{V}_2(\text{PO}_4)_3$ powders are generally prepared by solid-state reactions under a reducing atmosphere, requiring harsh reaction conditions [5-7]. Therefore, the fine homogenous $\text{Li}_3\text{V}_2(\text{PO}_4)_3$ powders, required for good electrochemical performance, cannot be obtained from solid-state reactions.

Liquid solution methods, such as sol-gel and hydrothermal methods, have been used to prepare fine $\text{Li}_3\text{V}_2(\text{PO}_4)_3$ powders at low calcination temperatures due to the high degree of mixing of the metal components [8-12]. However, the preparation of $\text{Li}_3\text{V}_2(\text{PO}_4)_3$ powders with spherical particles for a high tab density is difficult by such methods. Spray pyrolysis process is advantageous for the preparation of fine, spherical particles for use as cathode powders [13-19]. However, high-quality $\text{Li}_3\text{V}_2(\text{PO}_4)_3$ powders have not been prepared under normal spray pyrolysis conditions, even after post-treatment under a reducing atmosphere. The preparation conditions, such as the gas atmosphere, temperature, carrier gas flow rate, can affect the formation of $\text{Li}_3\text{V}_2(\text{PO}_4)_3$ by spray pyrolysis and this study reports their effects on $\text{Li}_3\text{V}_2(\text{PO}_4)_3$ cathode powders.

Experimental procedure

$\text{Li}_3\text{V}_2(\text{PO}_4)_3$ powders were prepared by ultrasonic spray

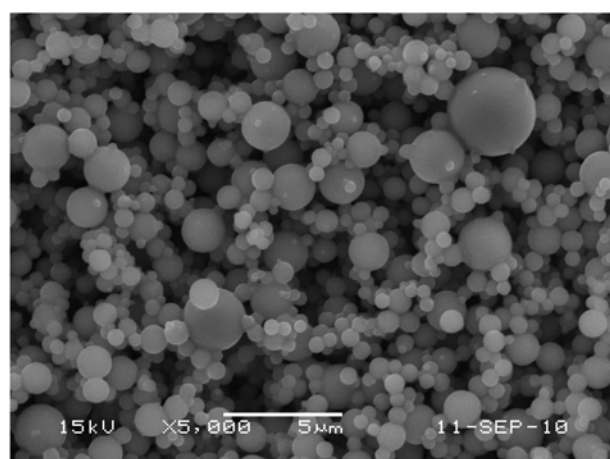
pyrolysis under various conditions. A 1.7 MHz ultrasonic spray generator with six vibrators was used to generate a large amount of droplets. Precursor solutions were prepared by dissolving lithium carbonate, vanadium oxide, and ammonium dihydrogen phosphate at the stoichiometric ratio of 3:2:3. The lithium component of the spray solution exceeded 15% of the stoichiometric amount to facilitate the formation of the $\text{Li}_3\text{V}_2(\text{PO}_4)_3$ powders. The reactor temperatures varied between 1100 and 1500 °C. The powders were prepared under air, N_2 and a 10% H_2/N_2 reducing gas atmosphere. The flow rate of the carrier gas varied between 10 and 30 L minute⁻¹. The concentration of the spray solution was 0.25 M.

The crystal structures of the precursor and the post-treated powders were investigated by X-ray diffractometry (XRD; Rigaku DMAX-33). Their morphologies were investigated by scanning electron microscopy (SEM; Jeol JSM-6060). Cathodes were prepared from mixtures of 12 mg $\text{Li}_3\text{V}_2(\text{PO}_4)_3$ and 4 mg TAB, which comprised 3.2 mg teflonized acetylene black and 0.8 mg binder. Lithium metal anodes and microporous polypropylene film separators were used. The electrolyte was 1 M LiPF_6 in a 1:1 mixture by volume of EC/DEC. The charge/discharge characteristics of the samples were measured by cycling at potentials of 3.0 - 4.8 V at a constant current density of 0.1 C using 2032-type coin cells.

Results and discussion

The morphologies of the precursor and the post-treated powders produced by spray pyrolysis under different atmospheres are shown in Figs. 1 and 2. The temperature of the reactor and the flow rate of the carrier gas were 1300 °C and 20 L minute⁻¹, respectively. The precursor

*Corresponding author:
Tel : +82-2-2049-6010
Fax: +82-2-458-3504
E-mail: yckang@konkuk.ac.kr



(a) air

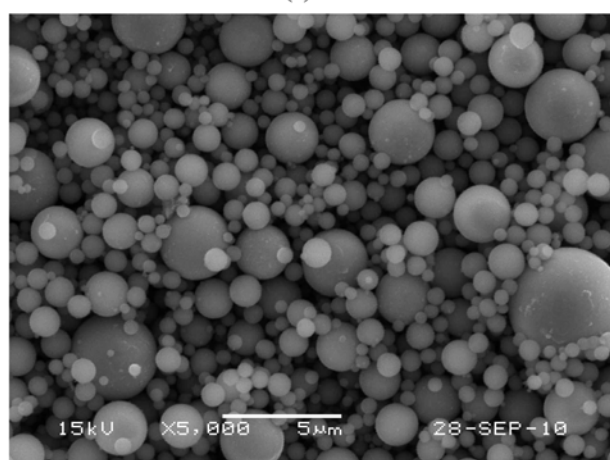
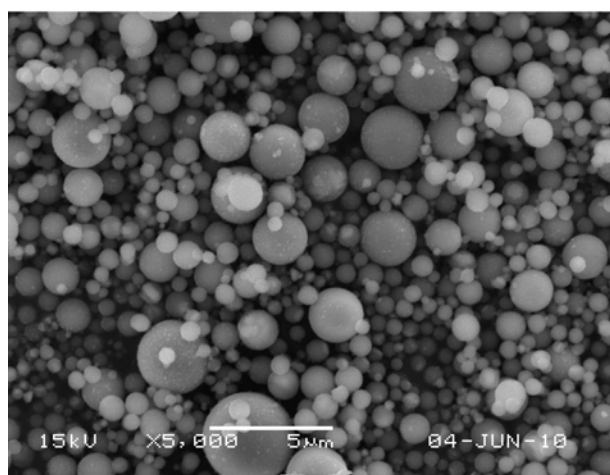
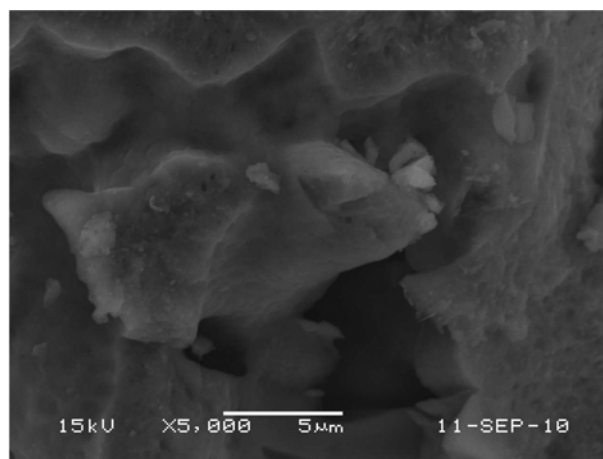
(b) N_2 (c) 10% H_2/N_2

Fig. 1. SEM images of the precursor powders prepared by spray pyrolysis with various gas atmospheres.

powders all showed similar morphologies irrespective of the preparation atmosphere. The submicrometre, spherical particles formed because each particle was prepared from one droplet. Post-treatment of the powders at 700 °C under a reducing atmosphere resulted in different morphologies according to the



(a) air

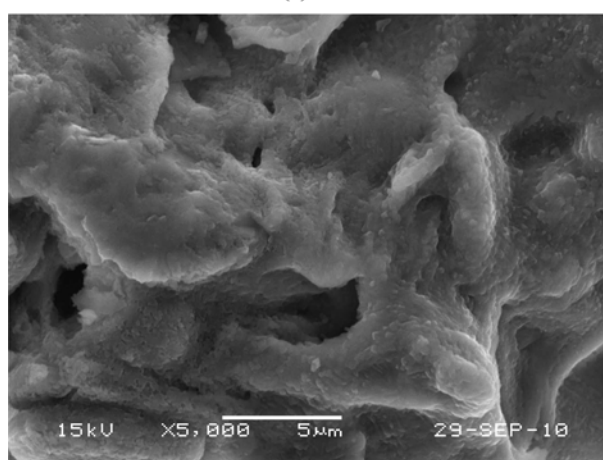
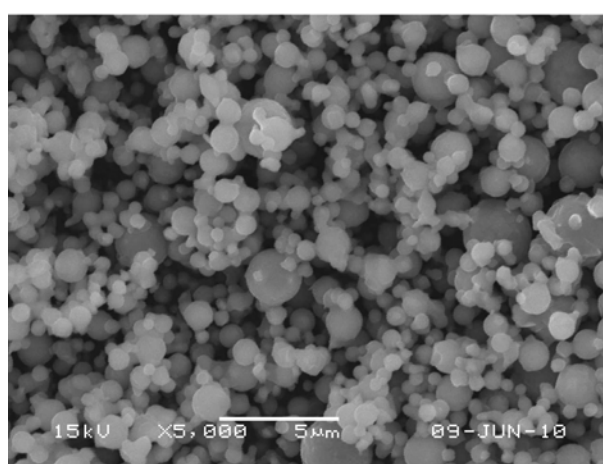
(b) N_2 (c) 10% H_2/N_2

Fig. 2. SEM images of the post-treated powders prepared by spray pyrolysis with various gas atmospheres.

preparation atmosphere of the precursors. Powders prepared under air and N_2 atmospheres melted during post-treatment and showed an irregular shape. Particles prepared under a 10% H_2/N_2 reducing gas atmosphere maintained their spherical morphology and submicrometre size after post-treatment. Figure 3 shows XRD patterns

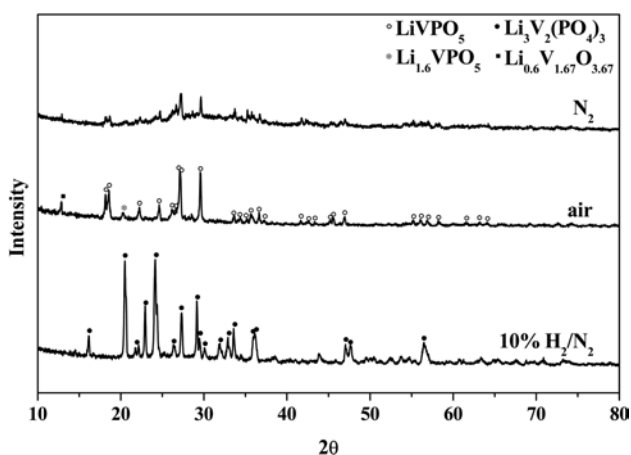


Fig. 3. XRD patterns of the post-treated powders prepared by spray pyrolysis with various gas atmospheres.

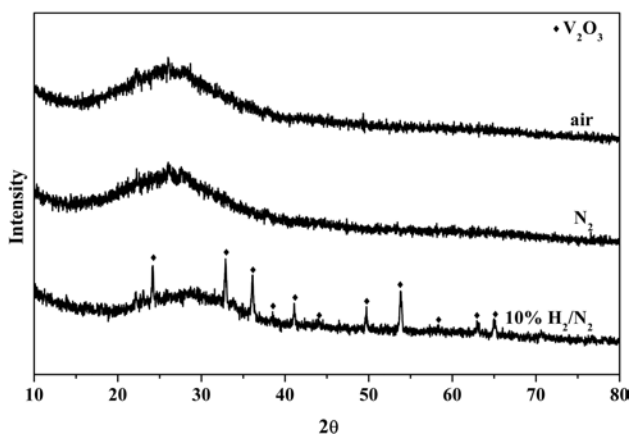


Fig. 4. XRD patterns of the precursor powders prepared by spray pyrolysis with various gas atmospheres.

of the post-treated powders. The powders obtained from precursors prepared under air and N_2 atmospheres showed mainly the $LiVPO_5$ crystal structure with small impurity peaks of $Li_{1.6}VPO_5$. The powders obtained from the precursor prepared under a 10% H_2/N_2 reducing gas atmosphere showed a pure crystal structure of $Li_3V_2(PO_4)_3$. Figure 4 shows the XRD patterns of the precursor powders prepared under different atmospheres. The precursor powders prepared under a 10% H_2/N_2 gas atmosphere showed peaks attributable to V_2O_5 ; peaks of Li and P components were not observed. On the other hand, the precursor powders prepared under air and N_2 were amorphous. The formation of different precursor intermediates under different atmospheres affected the formation of the $Li_3V_2(PO_4)_3$ phase during subsequent post-treatment.

Figure 5 shows little variation of the morphologies of precursor powders prepared at various temperatures under a 10% H_2/N_2 reducing gas atmosphere. The flow rate of the carrier gas was 20 L minute^{-1} . Post-treatment at 700°C resulted in different morphologies according to the preparation temperatures (Fig. 6). Powders prepared at low temperatures (below 1200°C) melted during later post-treatment and showed aggregated morphologies (Fig. 6 (a) and (b)). The particles obtained at above 1400°C were slightly aggregated and showed irregular morphologies. Figures 2 and 6 show that the optimum preparation temperature of the precursors to obtain spherical $Li_3V_2(PO_4)_3$ particles after post-treatment was 1300°C . Figure 7 shows XRD patterns of the precursor powders prepared at various temperatures under a 10% H_2/N_2 reducing gas atmosphere. Precursors prepared at below 1200°C showed the main peaks of

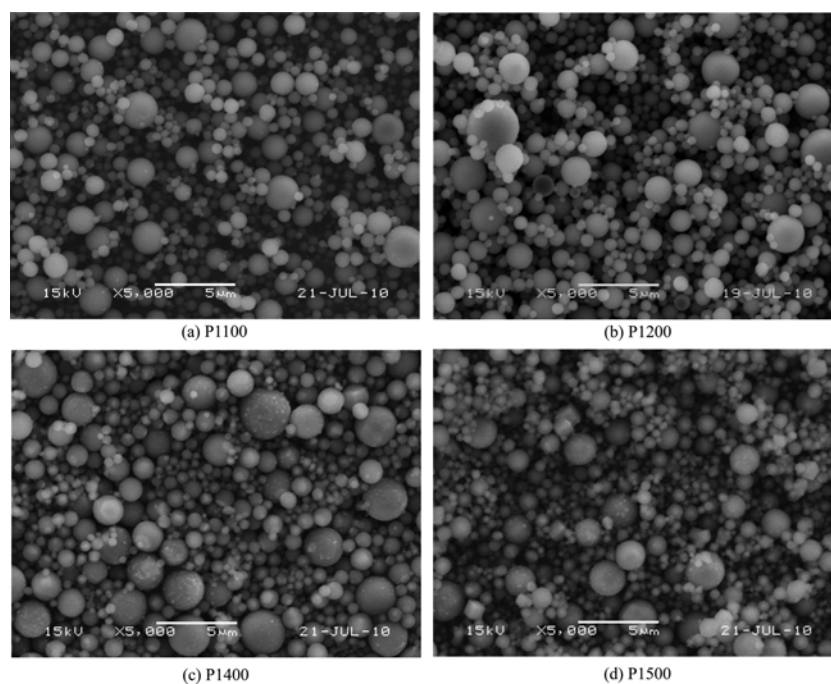


Fig. 5. SEM images of the precursor powders prepared by spray pyrolysis at various temperatures.

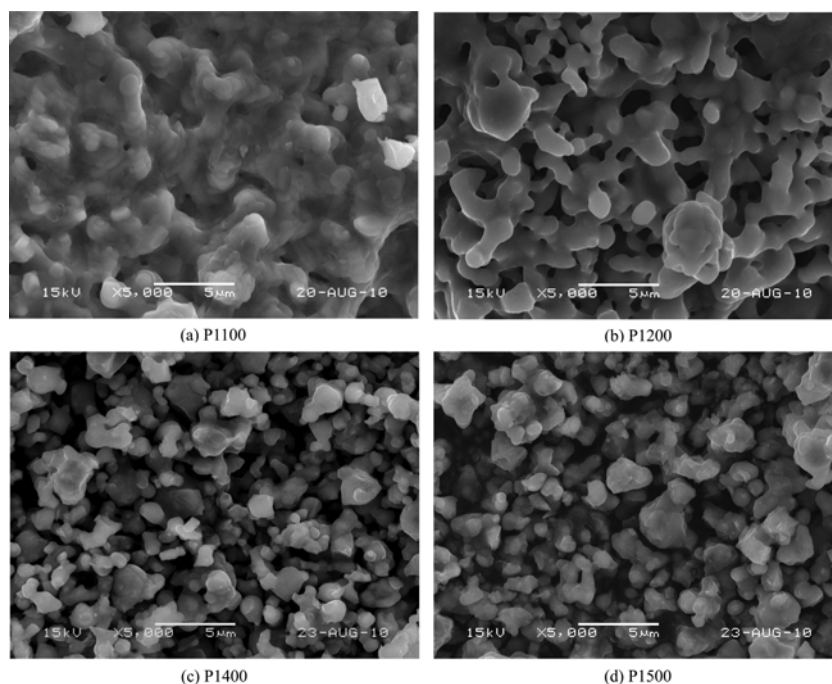


Fig. 6. SEM images of the post-treated powders prepared by spray pyrolysis at various temperatures.

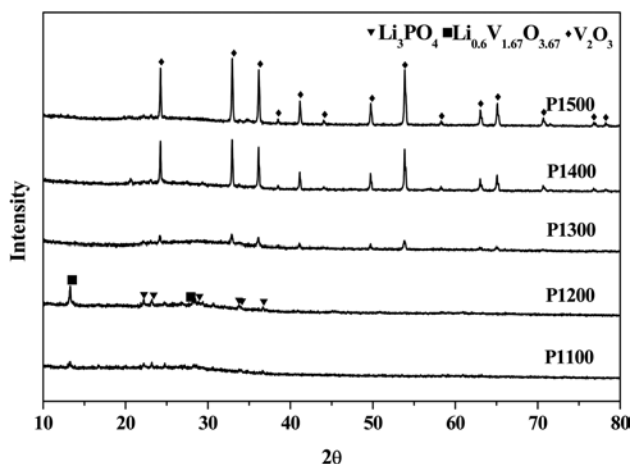


Fig. 7. XRD patterns of the precursor powders prepared by spray pyrolysis at various temperatures.

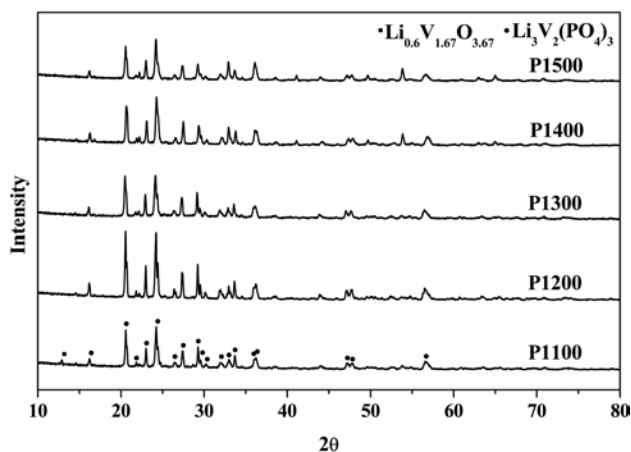
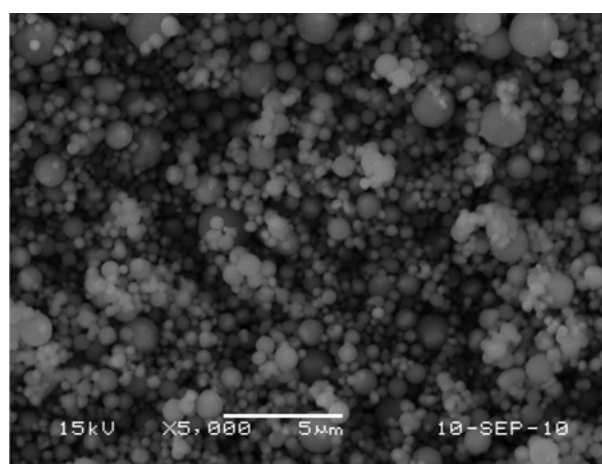
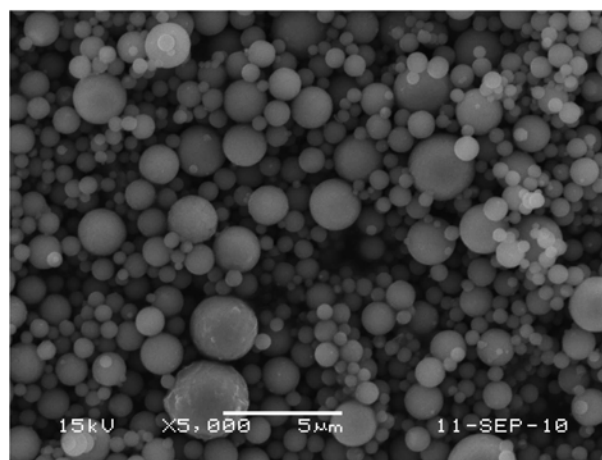


Fig. 8. XRD patterns of the post-treated powders prepared by spray pyrolysis at various temperatures.



(a) 10 L minute⁻¹



(b) 30 L minute⁻¹

Fig. 9. SEM images of the precursor powders prepared by spray pyrolysis at various flow rate.

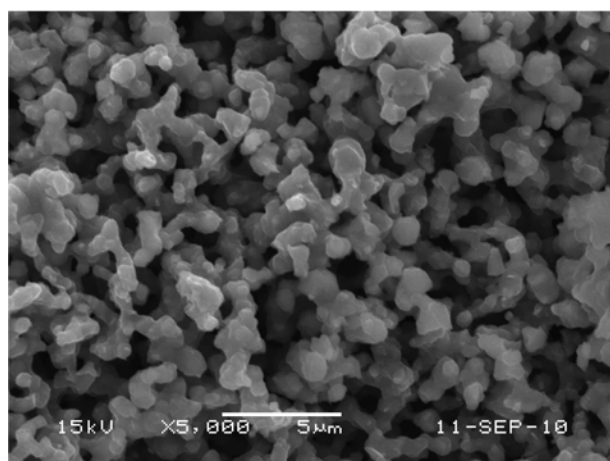
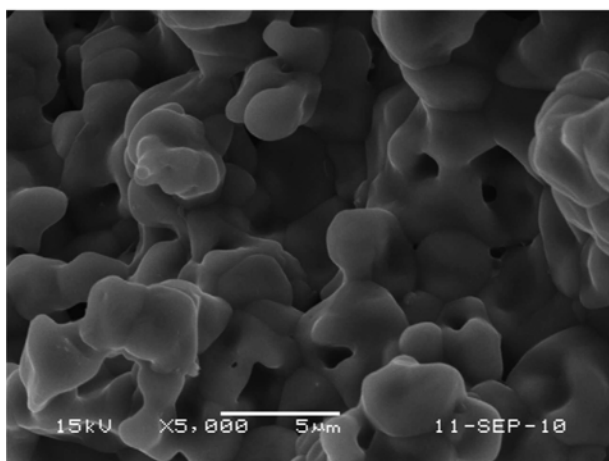
(a) 10 L minute⁻¹(b) 30 L minute⁻¹

Fig. 10. SEM images of the post-treated powders prepared by spray pyrolysis at various flow rate.

Li_3PO_4 and $\text{Li}_{0.6}\text{V}_{1.67}\text{O}_{3.67}$. The XRD patterns of precursors prepared at above 1300 °C showed the main peaks of V_2O_3 . Figure 8 shows the XRD patterns of the post-treated powders shown in Fig. 6. The powders obtained from precursors prepared at above 1200 °C were phase pure $\text{Li}_3\text{V}_2(\text{PO}_4)_3$. The powders obtained from the precursor prepared at 1100 °C showed the main peaks of $\text{Li}_3\text{V}_2(\text{PO}_4)_3$ and a small impurity peak of $\text{Li}_{0.6}\text{V}_{1.67}\text{O}_{3.67}$. Phase pure $\text{Li}_3\text{V}_2(\text{PO}_4)_3$ powders of fine and spherical particles were prepared by spray pyrolysis at high temperatures under a reducing atmosphere.

The flow rate of the carrier gas also affected the morphologies of the $\text{Li}_3\text{V}_2(\text{PO}_4)_3$ powders (Figs. 9 and 10). The precursors were prepared at 1300 °C under a 10 % H_2/N_2 reducing gas atmosphere; they were then post-treated at 700 °C. Increasing the carrier gas flow rate increased the mean particle size of the precursors because of increased rates of drying and decomposition of the droplets. Figures 2 and 10 show that the optimum flow rate of the carrier gas to obtain fine,

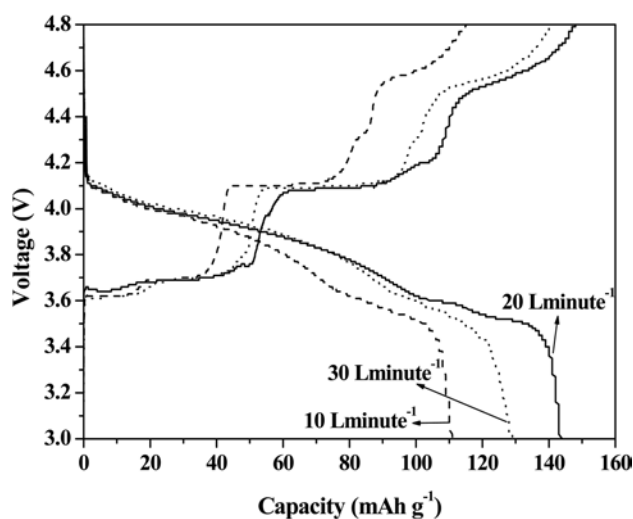


Fig. 11. Initial charge/discharge curves of the post-treated powders prepared by spray pyrolysis at various flow rates.

spherical $\text{Li}_3\text{V}_2(\text{PO}_4)_3$ particles was 20 L minute⁻¹. However, the optimum carrier gas flow rate can vary according to the size of the reactor.

Figure 11 shows the initial charge/discharge curves of the $\text{Li}_3\text{V}_2(\text{PO}_4)_3$ powders prepared at different carrier gas flow rates at a constant current density of 0.1 C over the potential range of 3.0–4.8 V. The charge and discharge curves of the powders were not greatly affected by the flow rate of the carrier gas. During charging, four plateaus at *ca.* 3.62, 3.70, 4.08, and 4.55 V were observed, corresponding to phase transitions between $\text{Li}_x\text{V}_2(\text{PO}_4)_3$ ($x = 3.0, 2.5, 2.0, 1.0$ and 0) [20]. $\text{Li}_3\text{V}_2(\text{PO}_4)_3$ powder produced from the precursor prepared with a carrier gas flow rate of 20 L minute⁻¹ had the maximum initial discharge capacity of 144 mAhg^{-1} . Larger and aggregated particles (Fig. 10) led to decreased discharge capacities.

Conclusions

The effects of the preparation conditions on the properties of $\text{Li}_3\text{V}_2(\text{PO}_4)_3$ powders prepared by spray pyrolysis were investigated. Post-treated powders obtained under the optimal preparation conditions comprised spherical and phase pure $\text{Li}_3\text{V}_2(\text{PO}_4)_3$ particles. The initial discharge capacities of the $\text{Li}_3\text{V}_2(\text{PO}_4)_3$ powders were affected by the preparation conditions of the precursors. The $\text{Li}_3\text{V}_2(\text{PO}_4)_3$ powders prepared at the optimum preparation conditions had a high discharge capacity.

Acknowledgement

This research was supported by Basic Science Research Program through the National Research Foundation of Korea (NRF) funded by the Ministry of Education, Science and Technology (2012002382). This study was also supported by Seoul R&BD Program

(WR090671). This study was also supported by a grant (M2009010025) from the Fundamental R&D Program for Core Technology of Materials funded by the Ministry of Knowledge Economy (MKE), Republic of Korea.

References

1. S.C. Yin, P.S. Strobel, H. Grondey and L.F. Nazar, *Chem. Mater.* 16 (2004) 1456-1465.
2. D. Morgan, G. Ceder, M.Y. Saidi, J. Barker, J. Swoyer, H. Huang and G. Adamson, *J. Power Sources* 119 (2003) 755-759.
3. J. Barker, M.Y. Saidi and J.L. Swoyer, *J. Electrochem. Soc.* 150 (2003) A684-A688.
4. Y. Hu and Y.H. Liu, *Mater. Chem. Phys.* 90 (2005) 255-261.
5. M.Y. Saidi, J. Barker, H. Huang, J.L. Swoyer and G. Adamson, *Electrochem. Solid-State Lett.* 5 (2002) A149-A151.
6. P. Fu, Y. Zhao, Y. Dong, X. An and G. Shen, *J. Power Sources* 162 (2006) 651-657.
7. P. Fu, Y. Zhao, Y. Dong, X. An and G. Shen, *Electrochim. Acta* 52 (2006) 1003-1008.
8. H. Huang, S.C. Yin, T. Kerr, N. Taylor and L.F. Nazar, *Adv. Mater.* 14 (2002) 1525-1528.
9. Y. Li, Z. Zhou, M. Ren, X. Gao and J. Yan, *Electrochim. Acta* 51 (2006) 6498-6502.
10. X.J. Zhu, Y.X. Liu, L.M. Geng and L.B. Chen, *J. Power Sources* 184 (2008) 578-582.
11. P. Fu, Y. Zhao, X. An, Y. Dong and X. Hou, *Electrochim. Acta* 52 (2007) 5281-5285.
12. C. Chang, J. Xiang, X. Shi, X. Han, L. Yuan and J. Sun, *Electrochim. Acta* 54 (2008) 623-627.
13. S.H. Ju, H.C. Jang and Y.C. Kang, *Electrochim. Acta* 52 (2007) 7286-7292.
14. I. Taniguchi, C.K. Lim, D. Song and M. Wakihara, *Solid State Ionics* 146 (2002) 239-247.
15. Z. Bakenov and I. Taniguchi, *Solid State Ionics* 176 (2005) 1027-1034.
16. I. Taniguchi, D. Song and M. Wakihara, *J. Power Sources* 109 (2002) 333-339.
17. S.H. Ju and Y.C. Kang, *Mater. Chem. Phys.* 126 (2011) 133-137.
18. S.H. Ju and Y.C. Kang, *J. Power Sources* 195 (2010) 4327-4331.
19. S.H. Ju and Y.C. Kang, *Electrochim. Acta* 55 (2010) 6088-6092.
20. X.H. Rui, C. Li and C.H. Chen, *Electrochim. Acta* 54 (2009) 3374-3380.